

Mathematical Modelling of Arterial Constriction in the Presence of Blood Diseases

¹Tivde, T., ²Ochayi, A. and ³Iorkua, M.

^{1,2}Department of Mathematics/Statistics/Computer Science, College of Science Federal University of Agriculture, Makurdi, Nigeria

³Department of Mathematics and Statistics, Benue State Polytechnic, Ugbokolo, Nigeria

Abstract:

Background: The Study is based on mathematical modelling of biofluids using the fundamental physical principles of fluid flow such as mass is conserved, Newton's second law and energy is conserved. These principles are used in the derivation of the blood flow models under consideration. The problem is investigated by using two different fluids. The result for resistance to flow across the length of the artery is obtained.

Materials and Methods: A mathematical model of a generalized Power-law blood and Casson-fluid flow through a stenosed artery is considered. This mathematical model is proposed and analyzed by studying the non-Newtonian flow of blood through a constricted (a diseased or stenosed) arterial segment. The solution of the models was obtained by direct integration.

Results: It has been observed that increase or decrease in resistance to flow in both the fluids depends on the height of the stenosis. Because of non-Newtonian behaviour of blood, these variations are less than that of Newtonian fluid. **Conclusion:** The graphical analysis of the variants of resistance to flow at maximum height of the stenosis is compared with a known investigation. Leaving reasonable recommendations on the blood flow pattern in the presence of diseases.

Key Words: Stenosis, Stenosed Artery, Arterial Constriction, Power-law blood flow, Casson-fluid flow, Newtonian fluid

Date of Submission: 05-02-2021

Date of acceptance: 19-02-2021

I. Introduction

One of the leading causes of deaths in the world is due to heart diseases, and the most commonly heard names among the same are ischemia, atherosclerosis, and angina pectoris. Ischemia is the deficiency of the oxygen in a part of the body, usually temporary. It can be due to a constriction (stenosis) or obstruction in the blood vessel supplying that part. Atherosclerosis is a type of arteriosclerosis. It comes from the Greek words athero (meaning gruel or paste) and sclerosis (hardness). It involves deposits of fatty substances, cholesterol, cellular waste products, calcium and fibrin (a clothing material in the blood) in the inner lining of an artery. The build-up that results is called plaque. Plaque may partially or totally block the channel (artery) through which blood flows. The major two things that can happen where plaque occurs are (i) bleeding (hemorrhage) into the plaque, and (ii) formation of a blood clot (thrombus) on the plaque's surface. If either of these occurs and blocks the entire artery, a heart attack or stroke may result. Atherosclerosis affects large and medium sized arteries [11]. The type of artery where the plaque develops varies with person to person.

In cardiac-related problems, the affected arteries get hardened as a result of accumulation of fatty substances inside the lumen or because of formation of plaques as a result of hemorrhage. As the disease gets progressed, the arteries/arteriole gets constricted. The flow behaviour in the stenosed artery is quite different from the one in the normal arteries [3], [11], [12]. Also, stresses and resistance to flow are much higher in stenosed arteries in comparison to the normal ones. Having knowledge on flow parameters, such as velocity, flow rate, pressure drop will aid bio-medical engineers in developing bio-medical instruments for treatment (surgical) modalities. Hence fluid mechanics aspect of arterial stenosis have received a considerable attention in the recent past. In view of its importance, a fluid mechanics aspect of arterial stenosis has been undertaken in the present studies.

While modelling blood flow in a stenosed tube, it was initially assumed by [1] that, the flow obeys Newtonian hypothesis and the flow variables have been computed by using basic Navier–Stoke Equations. Later, the model has been extended by assuming that, it obeys non-Newtonian hypothesis and developed the model for either Casson-fluid or for Power-law fluids, and showed that, under low shear rates, the model could be best described by this representation. During constriction (stenosis), the lumen of an artery gets considerably

reduced thereby, size effects (particle size (mainly red blood cells) to tube diameter ratio) influences the flow characteristics significantly.

The problem of atherosclerosis cut across all genders worldwide but mostly found in adult. It involves deposits of fatty substances in the internal lining of an artery. The development of an obstruction in the artery can lead to serious circulatory disorders. In this situation, the flow behaviour is quite different from normal artery. It has caused a lot of havoc to human lives thereby pushing many to their early graves. If appropriate measure is not taken to curtail the menace of this disease, many lives will still be affected.

It was well learnt from [4] that the presence of stenosis in the arterial channel is particularly dangerous in the coronary and carotid arteries due to the critical oxygen requirement of the heart and brain. Blood flow study is the measuring of the blood pressure and finding the flow through the blood vessel. This study is important for human health. Most of the researches study the blood flow in the arteries and veins. One of the motivations to study the blood flow was to understand the conditions that may contribute to high blood pressure [5].

In the same way, [5] indicated that one of the reasons people have hypertension is that the blood vessel becomes narrow. Blood is non-Newtonian fluid and to model such fluid is very complicated. In this problem, blood is assumed to be a Newtonian fluid. Even though this will make the problem much simpler, it still is valid since blood in a large vessel acts almost like a Newtonian fluid. In order to model this problem, Navier-Stokes equations will be used to derive the governing equations that represent this problem.

The effects of stenosis on the blood flow through the artery with mild stenosis treating blood as a non-Newtonian fluid was studied by [6] revealing that stenosis has no well-defined configuration. In general, complex three-dimensional flow patterns have been developed near the stenosis, which are virtually impossible to analyse.

The analyses of blood as a Power-law fluid and a Casson-fluid in an artery having composite shape of mild stenosis is carried out by [1]. This study extends the model of [1] by considering multiple stenoses having composite shape of severe stenosis which may result into arterial occlusion.

The investigations of blood flow through arteries are of considerable importance in many cardiovascular diseases. Hence the mathematical modelling of this type of flows can be very useful. It is noted that, [2] studied the effects of stenosis on the blood flow through the artery with mild stenosis treating blood as a non-Newtonian fluid. It is obvious that stenosis has no well-defined configuration and their result is in line with [3]. In general, complex three dimensional flow patterns have been developed near the stenosis, which are virtually impossible to analyse [1]. analysed blood as a Power-law fluid and a Casson-fluid in an artery having composite shape of mild stenosis. In our study we have extended the model of [1] by considering multiple stenoses having composite shape of severe stenosis which may result into arterial occlusion.

The aim of this research work is to model the arterial restriction in the presence of blood diseases. The specific objectives are to; formulate mathematical model of blood flow via a severely stenosed artery, analyse blood as a Power-law fluid and a Casson-fluid in a constricted artery, determine the impact of arterial constriction on lumen and diameter of the artery, determine the blood flow index on the arterial wall shear stress as well as resistance to the flow of blood, find out the flow pattern in normal artery and compared with a severely stenosed arterial channel under consideration and analyse the velocity profile, flow rate, wall shear stress, and resistance of the blood flow for different parameters.

II. Material and Methods

The Study is based on mathematical modelling of biofluids using the fundamental physical principles of fluid flow such as mass is conserved, Newton's second law and energy is conserved. These principles are used in the derivation of the blood flow models under consideration. A mathematical model of a generalized Power-law blood and Casson-fluid flow through a stenosed artery is considered. This mathematical model is proposed and analyzed by studying the non-Newtonian flow of blood through a constricted (a diseased or stenosed) arterial segment.

Model Formulation

This very section of the research paper presents among many others; the assumptions of the model, model parameters and variables, geometric representation of the model flow process (a typical representation of a tapered artery, structure of the artery showing the flow pattern of blood in a truncated artery, a cross-section of an artery with boundary later occluded at some region, a cross-section of an artery with boundary later occluded at some region showing how the boundary layer grows gradually until occluded as the radius narrowed a geometric representation of arterial system based on power-law, a geometric representation of arterial system based on Casson-fluid).

Assumptions of the model

In the formulation of the model, it is assumed that

1. The blood flowing in the tube is a suspension of red cells in plasma and the fluid is incompressible, non-Newtonian and viscous.
2. The formation of stenosis in a uniform circular tube is considered to be axisymmetric.
3. For the development of model geometry of the stenosis in the arterial segment can be described same as [1].
4. The arterial channel is considered to be tapered in shape.
5. A symmetric core layer exists around the axis

Model parameters and variables

The model parameters and variables are as shown in Table 1;

Table 1 Table show the variables and parameters of the model with their meanings

Parameters/variables	Meanings
R_0	Radius of the non-stenotic region
$R(z)$	Radius of the stenotic region
L	The length of the artery
L_0	The length of the stenosis
D	Location of stenosis
P_i	Inlet fluid pressure
p_0	Outlet fluid pressure
δ_h	Maximum height of the stenosis
τ	shear stress,
w	axial velocity,
Q	volumetric flow rate
τ_R	shear stress at the wall
M	consistency index
N	flow behaviour index.
λ_N	resistance to flow
$f(\tau)$	general function for the given fluid (blood).

The geometric representation of the model flow process

We first considered the structure of the artery and state that the smaller muscular arteries range from 40 – 300 μm in diameter, and those that are 40 μm in diameter have approximately three or four layers of smooth muscle in their tunica media, whereas arteries that are 300 μm across have essentially the same structure as the larger muscle arteries. They are adopted for vasodilation and vasoconstriction. The arterioles transport blood from small arteries to capillaries and are the smallest arteries in which the three tunics can be identified. They range from 40 μm to as small as 9 μm in diameter this agrees with [9]. With this, we can draw a general structure of the artery geometrically being slowly varying in diameter (tapered in shape) as in *Figure 1.0*:

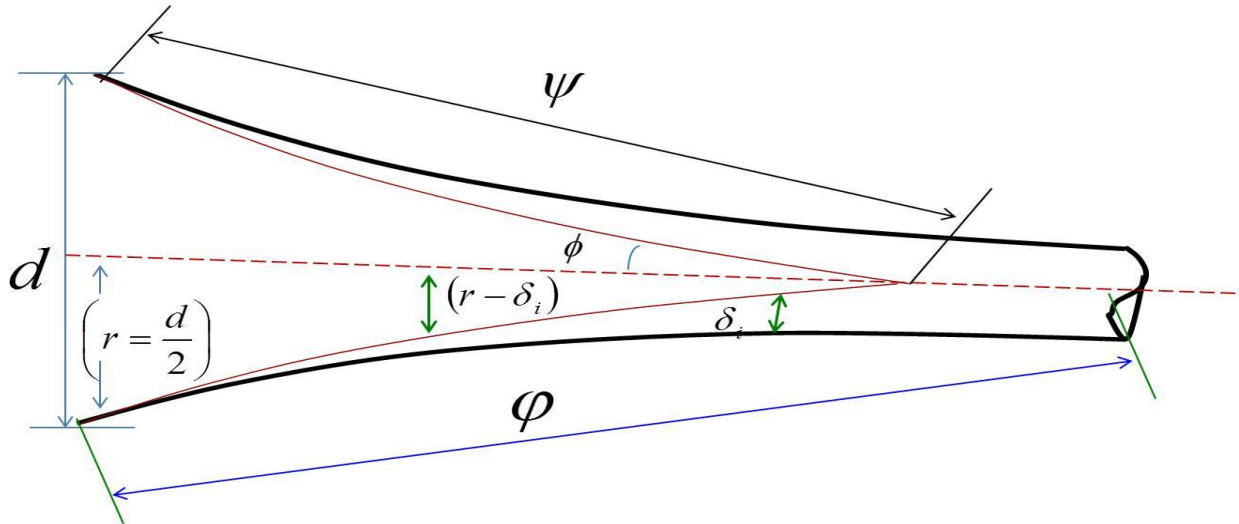


Figure 6: A cross-section of an artery with boundary later and occluded at some region showing how the boundary layer grows gradually until occluded as the radius narrowed [11].

A critical study of our Figure 5 has shown that, the flow velocity of blood is constant across the converging part of the artery at L i.e. the flow is laminar and turbulent at T . As blood flows down the artery to the body, the arterial walls may cause the growth of boundary layer with thickness δ_i [11]. We have considered a short truncation of the artery which is almost straight and hence have the geometric representation of the arterial system based on power-law as shown in Figure 6:

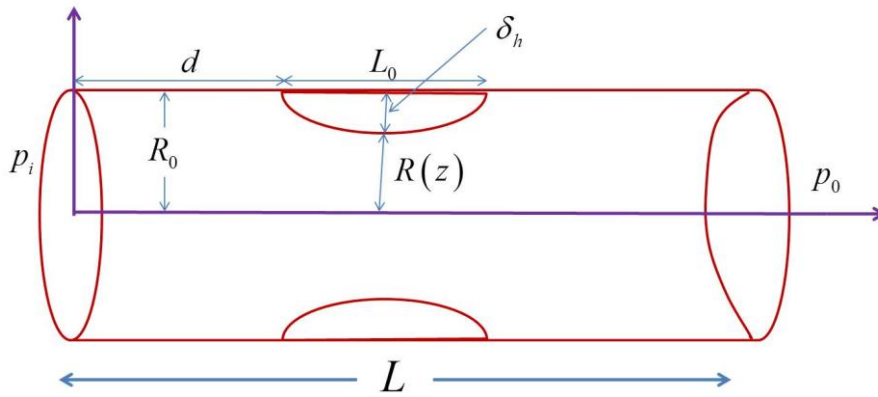


Figure 7a: A geometric representation of arterial system showing the flow process based on power-law

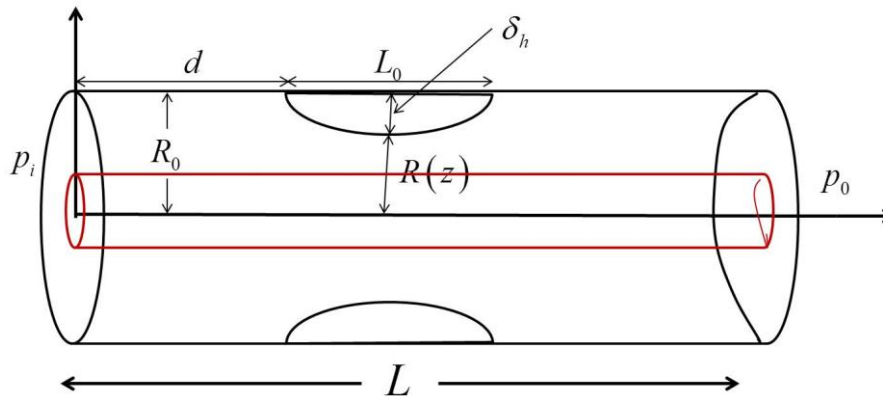


Figure 8b: A geometric representation of arterial system based on Casson- Fluid

The Governing model for the system

The governing equations here are given by the existing and the new models derived and presented here.

The existing model

Following from the assumptions of the model, the development of model geometry of the stenosis in the arterial segment can be described similar to that of [13]. Using the schematic diagram for Power-Law, we have;

$$R(z) = \begin{cases} R_0 - \frac{2\delta_h}{L_0}(z-d) & d \leq z \leq d + \frac{L_0}{2} \\ R_0 - \frac{\delta_h}{2} \left[1 + \cos\left(\frac{2\pi}{L_0}\left(z-d-\frac{L_0}{2}\right)\right) \right] & d \leq z \leq d + \frac{L_0}{2} \\ R_0 & \text{Otherwise} \end{cases} \quad (1a)$$

The height of stenosis is assumed to be much smaller in comparison to the radius R_0 that is $\delta_h \ll R_0$.

The general constitutive equation can be written as,

$$\left(-\frac{dw}{dr}\right) = f(\tau) \quad (1b)$$

where τ is the shear stress, w is the axial velocity, $\frac{dw}{dr}$ is the shear rate and $f(\tau)$ is general function for the given fluid. Following [13], the volumetric flow rate Q is given by

$$Q = \frac{\pi R^3}{\tau_R^3} \int_0^{\tau_R} \tau^2 f(\tau) d\tau \quad (2)$$

where

$$\tau = -\frac{1}{2}r \frac{dp}{dz} \quad \text{and} \quad \tau_R = -\frac{1}{2}R \frac{dp}{dz} \quad (3)$$

Here $\frac{dp}{dz}$ is the pressure gradient and τ_R is the shear stress at the wall.

Existing model based on power-law

In power-law fluids, $f(\tau)$ is given by,

$$\left(-\frac{dw}{dr}\right) = \left(\frac{\tau}{m}\right)^{\frac{1}{n}} \quad (4)$$

where m is consistency and n is flow behaviour index. Using equation (3) and (4) in equation (2), we get

$$\frac{dp}{dz} = -2m \left(\frac{3n+1}{n\pi}Q\right)^n \frac{1}{R^{(3n+1)}} \quad (5)$$

Subject to the conditions; the conditions $p = p_i$ at $z = 0$ and $p = p_0$ at $z = L$.

Existing model based on Casson – fluid model

The general constitutive equation is given by,

$$\left. \begin{aligned} \left(-\frac{dw}{dr}\right)^{\frac{1}{2}} &= \frac{r^{\frac{1}{2}} - r_0^{\frac{1}{2}}}{n} ; \tau \geq r_0 \\ \frac{dw}{dr} &= 0 ; \tau \leq r_0 \end{aligned} \right\} \quad (6)$$

where w is axial velocity, τ_0 is yield stress and η^2 is the viscosity of the fluid.

The new model

Following from the assumptions of the model, the development of model geometry of the stenosis in the arterial segment can be described similar to that of [13]. Using the schematic diagram for Power-Law, we have;

$$R(z) = \begin{cases} R_0 - \sum_{i=1}^n \left\{ r_i - \frac{2\delta_{hi}}{L_0}(z-d_i) \right\} & d_i \leq z \leq d_i + \frac{L_0}{2} \\ R_0 - \sum_{i=1}^n \left\{ \frac{\delta_{hi}}{2} \left[1 + \cos\left(\frac{2\pi}{L_0}\left(z-d_i-\frac{L_0}{2}\right)\right) \right] \right\} & d_i \leq z \leq d_i + \frac{L_0}{2} \\ R_0 & \text{Otherwise} \end{cases} \quad (7)$$

The fact that the height of stenosis is much smaller in comparison to the radius R_0 that is $\delta_h \ll R_0$.

Following the general constitutive equation given (1b) and adopting the volumetric flow rate Q

$$Q = \frac{\pi R^3}{\tau_R^3} \int_0^{\tau_R} \tau^2 f(\tau) d\tau \quad (8)$$

where

$$\tau = -\frac{1}{2}r \frac{dp}{dz} = -\frac{1}{2} \frac{dp}{dz} \sum_{i=1}^n \left\{ r_i - \frac{2\delta_{hi}}{L_0} (z-d_i) \right\} \tag{9}$$

and

$$\tau_R = -\frac{1}{2} \left\{ R_0 - \sum_{i=1}^n \left\{ r_i - \frac{2\delta_{hi}}{L_0} (z-d_i) \right\} \right\} \frac{dp}{dz} \tag{10}$$

where $\frac{dp}{dz}$ is the pressure gradient and τ_R is the shear stress at the wall of the tapered artery.

The new model based on power-law

In power-law fluids $f(\tau)$ is given by,

$$\left(-\frac{dw}{dr} \right) = \left(\frac{\tau}{m} \right)^{\frac{1}{n}} \tag{11}$$

where m is consistency and n is flow behaviour index. Using equation (3) and (4) in equation (2), we get

$$\frac{dp}{dz} = -2m \left(\frac{3n+1}{n\pi} Q \right)^n \frac{1}{R^{(3n+1)}} \tag{12}$$

Subject to the conditions; the conditions $p = p_i$ at $z = 0$ and $p = p_0$ at $z = L$ with R as in (1).

The new model based on casson – fluid model

The general constitutive equation is given by,

$$\left. \begin{aligned} \left(-\frac{dw}{dr} \right)^{\frac{1}{2}} &= \frac{\sum_{h,i} (r - \delta_{hi})^{\frac{1}{2}} - r_0^{\frac{1}{2}}}{n} ; \tau \geq r_0 \\ \frac{dw}{dr} &= 0 ; \tau \leq r_0 \end{aligned} \right\} \tag{13}$$

where w is axial velocity, τ_0 is yield stress and η^2 is the viscosity of the fluid.

Method of Solution

The solution will be obtained by direct integration applying the stated boundary conditions; $z = 0$ and $p = p_0$ at $z = L$.

Definition 1: If the function f is continuous on the interval $[a, b)$ and discontinuous at $x = b$, then

$$\int_a^b f(x)dx = \lim_{t \rightarrow b^-} \int_a^t f(x)dx.$$

We recall that a definite integral exists if the integrand is continuous on the closed interval $[a, b]$ of integration. Since the integrand f is continuous on the interval $[a, b)$, then it is continuous on the closed interval $[a, t]$ for all $a \leq t < b$. Thus, $\int_a^t f(x)dx$ exists for all $a \leq t < b$. Of course, if $t = a$, then since the function f is continuous at $t = a$, then the function f is defined at $t = a$ and $\int_a^a f(x)dx = 0$.

Definition 2: If the function f is continuous on the interval $(a, b]$ and discontinuous at $x = a$, then

$$\int_a^b f(x)dx = \lim_{t \rightarrow a^+} \int_t^b f(x)dx.$$

Since the integrand, f is continuous on the interval $(a, b]$, then it is continuous on the closed interval $[t, b]$ for all $a < t \leq b$. Thus, $\int_t^b f(x)dx$ exists for all $a < t \leq b$. Of course, if $t = a$, then since the function, f is continuous at $t = a$, then the function, f is defined at $t = a$ and $\int_a^a f(x)dx = 0$.

The integral $\int_a^b f(x)dx$ in the definitions above are also called improper integrals because of the integrand has a discontinuity on the closed interval $[a, b]$. If the limit in the definition exists, we say that the improper integral converges. If the limit does not exist, then we say that the improper integral diverges.

Definition 3: If the function f has a discontinuity at $x = c$ in the open interval (a, b) but is continuous elsewhere in the closed interval $[a, b]$, then

$$\int_a^b f(x)dx = \int_a^c f(x)dx + \int_c^b f(x)dx = \lim_{r \rightarrow c^-} \int_a^r f(x)dx + \lim_{t \rightarrow c^+} \int_t^b f(x)dx$$

provided that both of the improper integrals converge.

Theorem 1: Fundamental Theorem of Calculus

a) If $f(x)$ is continuous on $[a, b]$ and $F(x)$ is any antiderivative of $f(x)$, then

$$\int_a^b f(x)dx = F(b) - F(a). \text{ Alternative notation: } \int_a^b f(x)dx = F(x) \Big|_a^b$$

b) If $f(x)$ is continuous on $[a, b]$ and $F(x) = \int_a^x f(t)dt$, then $F'(x) = f(x)$ on $[a, b]$

a) **Proof: The Proof is as in [9].**

Method of solution for the model built based on power law

Now, integrating equation

$$\frac{D}{Dt} \int_V (\rho e + \frac{1}{2} \rho u \cdot u) dV = \int_S u P dS + \int_V u \rho f dV - \int_S q \cdot n dS$$

and using the conditions $p = p_i$ at $z = 0$ and $p = p_0$ at $z = L$, we get

$$p - p_0 = \left(2m \left(\frac{3n+1}{n\pi} Q \right)^n \frac{1}{R^{(3n+1)}} \right) \int_0^L \frac{dz}{(R/R_0)^{(3n+1)}} \tag{15}$$

where R/R_0 is given by equation (1a).

$$\lambda = \frac{p_i - p_0}{Q} \tag{16}$$

which on using equations (1a) and (15) gives,

$$\lambda = \left(2m \left(\frac{3n+1}{n\pi} Q \right)^n \frac{1}{Q^{(1-n)R^{(3n+1)}}} \right) \left[\int_0^d \frac{dz}{(R/R_0)^{(3n+1)}} + \int_d^{d+\frac{L_0}{2}} \frac{dz}{(R/R_0)^{(3n+1)}} + \int_{d+\frac{L_0}{2}}^{d+L_0} \frac{dz}{(R/R_0)^{(3n+1)}} + \int_{d+L_0}^L \frac{dz}{(R/R_0)^{(3n+1)}} \right] \tag{17}$$

In case of no stenosis the resistance to flow λ_N is given by.

$$\lambda_N = \left(2m \left(\frac{3n+1}{n\pi} Q \right)^n \frac{L}{QR^{(3n+1)}} \right) \tag{18}$$

From equations (17) and (18) we can find,

$$\bar{\lambda} = \frac{\lambda}{\lambda_N} = \frac{1}{L} \left[\int_0^d \frac{dz}{(R/R_0)^{(3n+1)}} + \int_{d+L_0}^L \frac{dz}{(R/R_0)^{(3n+1)}} + I_1 + I_2 \right] \tag{19}$$

where,

$$I_1 = \frac{dz}{(R/R_0)^{3n+1}} \tag{20}$$

and

$$I_2 = \int_d^{d+\frac{L_0}{2}} \frac{dz}{(R/R_0)^{3n+1}} \tag{21}$$

using equation (1a), we can find

$$I_1 = \frac{L_0}{2} \left[1 + \frac{3n+1}{2} \left(\frac{\delta_h}{R_0} \right) + \frac{(3n+1)(3n+2)}{6} \left(\frac{\delta_h}{R_0} \right)^2 + \dots \right] \tag{22}$$

$$I_2 = \frac{L_0}{2} \left[\frac{1}{3n!} \left(\frac{1}{\sqrt{a^2+b^2}} \right)^{(3n+1)} \sum_{s=0}^{3n} (-1)^s \frac{3n!(3n+1)!}{(s!)^2(3n-s)!} \left(\frac{-a+\sqrt{a^2-b^2}}{2\sqrt{a^2-b^2}} \right)^s \right] \tag{23}$$

where $a = 1 - \frac{\delta_h}{2R_0}$ and $b = \frac{\delta_h}{2R_0}$

using equation (22) and (23) in equation (19), we get

$$\bar{\lambda} = 1 - \frac{L_0}{2} + \frac{L_0}{2L} \left[\left(1 + \frac{3n+1}{2} \left(\frac{\delta_h}{R_0} \right) + \frac{(3n+1)(3n+2)}{6} \left(\frac{\delta_h}{R_0} \right)^2 + \dots \right) + \left(\frac{1}{3n!} \left(\frac{1}{\sqrt{a^2-b^2}} \right)^{(3n+1)} \sum_{s=0}^{3n} (-1)^s \frac{3n!(3n+1)!}{(s!)^3(3n-s)!} \left(\frac{-a+\sqrt{a^2-b^2}}{2\sqrt{a^2-b^2}} \right)^s \right) \right] \tag{24}$$

From the equations (12) and (14) we can obtain

$$\bar{\tau} = \frac{\tau_s}{\tau_N} = \frac{1}{\left(1 - \frac{\delta_h}{R_0} \right)^{3n}} \tag{25}$$

where τ_s is the value of τ_R at maximum height of stenosis and τ_N is the shear when there is no stenosis i.e. $\delta_h = 0$.

Method of solution for the model built based on casson – fluid model

In this case, it is assumed that a symmetric core layer exists around the axis as shown in Figure 3. As before, from equations (11), (12) and (23) we can find

$$\frac{dp}{dz} = -\frac{2}{R} \left[\frac{8}{7} \sqrt{T_0} + 2\eta \sqrt{\frac{Q}{\pi R^3}} \right]^2 \quad (26)$$

For small $T_0/T_R \ll 1$

Following same procedure as in Case I, we can find

$$\bar{\lambda} = 1 - \frac{L_0}{L} + \frac{L_0}{L(f+g+h)} [fG_1 + gG_2 + hG_3] \quad (27)$$

where

$$f = \frac{128}{49} \frac{\tau_0}{QR_0}, g = \frac{8\eta^2}{\pi R_0^4}, h = \frac{64\eta}{7R_0^{5/2}} \sqrt{\frac{\tau_0}{\pi Q}}$$

and

$$G_1 = \frac{1}{L_0} \int_d^{d+L_0} \frac{dz}{(R/R_0)}, G_2 = \frac{1}{L_0} \int_d^{d+L_0} \frac{dz}{(R/R_0)^{5/2}}, G_3 = \frac{1}{L_0} \int_d^{d+L_0} \frac{dz}{(R/R_0)^4}$$

Finding above integrals using equation (3.12) as follows:

$$G_1 = \left[1 + \frac{1}{2} \left(\frac{\delta_h}{R_0} \right) + \frac{17}{48} \left(\frac{\delta_h}{R_0} \right)^2 + \frac{9}{32} \left(\frac{\delta_h}{R_0} \right)^3 + \dots \right] \quad (28)$$

$$G_3 = \frac{1}{2} \left[\left(1 + 2 \left(\frac{\delta_h}{R_0} \right) + \frac{10}{3} \left(\frac{\delta_h}{R_0} \right)^2 + \dots \right) + \left(1 - \frac{\delta_h}{2R_0} \right) \left(1 - \frac{\delta_h}{R_0} + \frac{5}{8} \left(\frac{\delta_h}{R_0} \right)^2 \right) \left(1 - \frac{\delta_h}{R_0} \right)^{(-7/2)} \right] \quad (29)$$

$$G_3 = \frac{1}{2} \left[\left(1 + \frac{5}{4} \left(\frac{\delta_h}{R_0} \right) + \frac{35}{24} \left(\frac{\delta_h}{R_0} \right)^2 + \dots \right) + \left(1 + \frac{5}{4} \left(\frac{\delta_h}{R_0} \right) + \frac{35}{32} \left(\frac{\delta_h}{R_0} \right)^2 + \dots \right) \left(1 + \frac{35}{64} \left(\frac{\delta_h}{R_0} \right)^2 \left(1 + \left(\frac{\delta_h}{R_0} \right) + \frac{3}{4} \left(\frac{\delta_h}{R_0} \right)^2 + \dots \right) \right] \quad (30)$$

Equation (3.40) together with equations (29), (30) and (31) will give the value of $\bar{\lambda}$. When $\tau_0 = 0$, equation (28) becomes

$$\bar{\lambda} = 1 - \frac{L_0}{L} + \frac{L_0}{L} \left[\frac{1}{2} \left(1 + 2 \left(\frac{\delta_h}{R_0} \right) + \frac{16}{5} \left(\frac{\delta_h}{R_0} \right) + \dots \right) + \left(1 - \frac{\delta_h}{2R_0} \right) \left(1 - \frac{\delta_h}{R_0} + \frac{5}{4} \left(\frac{\delta_h}{R_0} \right)^2 \right) \left(1 - \frac{\delta_h}{R_0} \right)^{(-7/2)} \right] \quad (31)$$

Proceeding on the lines of the model I and using equations (1a), (3) and (17), the wall shear ratio is given as,

$$\bar{\tau} = \frac{1}{(f+g+h)} \left[f + \frac{g}{\left(1 - \frac{\delta_h}{R_0} \right)^3} + \frac{g}{\left(1 - \frac{\delta_h}{R_0} \right)^{\frac{3}{2}}} \right] \quad (32)$$

III. Result

The results of the study are presented in this chapter with the aid of graphs (Figures 8 – Figure 16). The graphs are plotted based both the Power-Law and Casson fluids by simulating the solutions, ((24), (25), (32) and (33)) of the models.

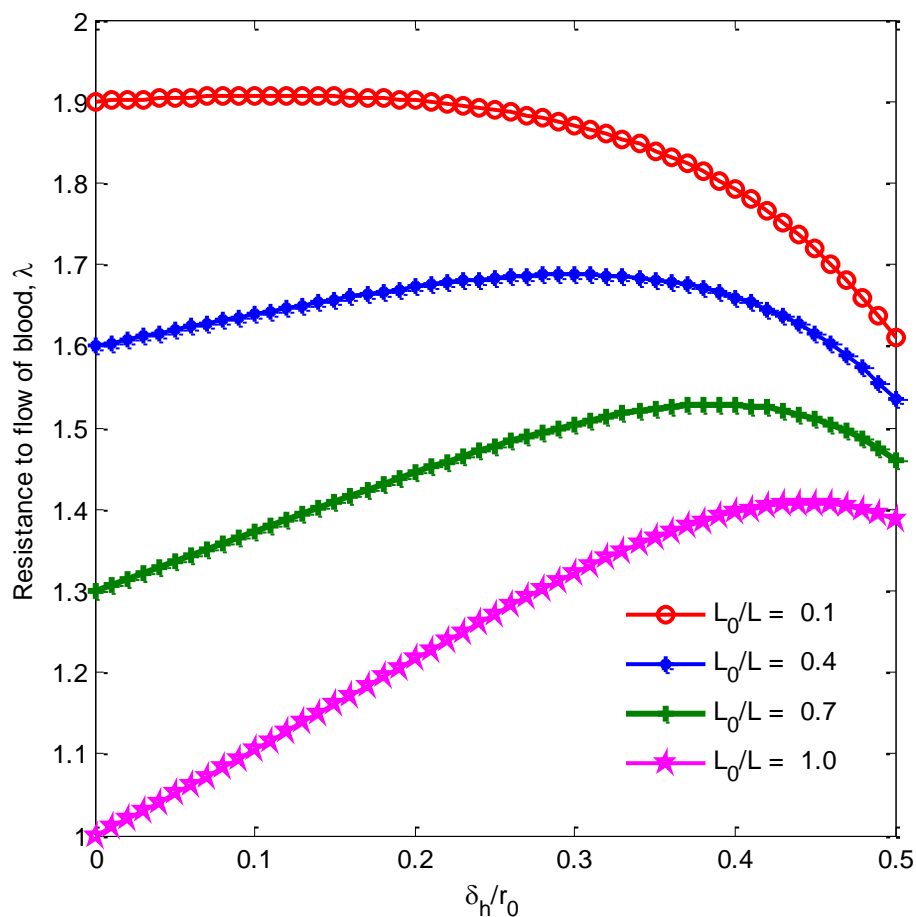


Figure 8: Variation of resistance to flow, $\bar{\lambda}$ with $\frac{\delta_h}{R_0}$ for values of $L_0/L = 0.1, 0.4, 0.7$ and 1.0 based on power law

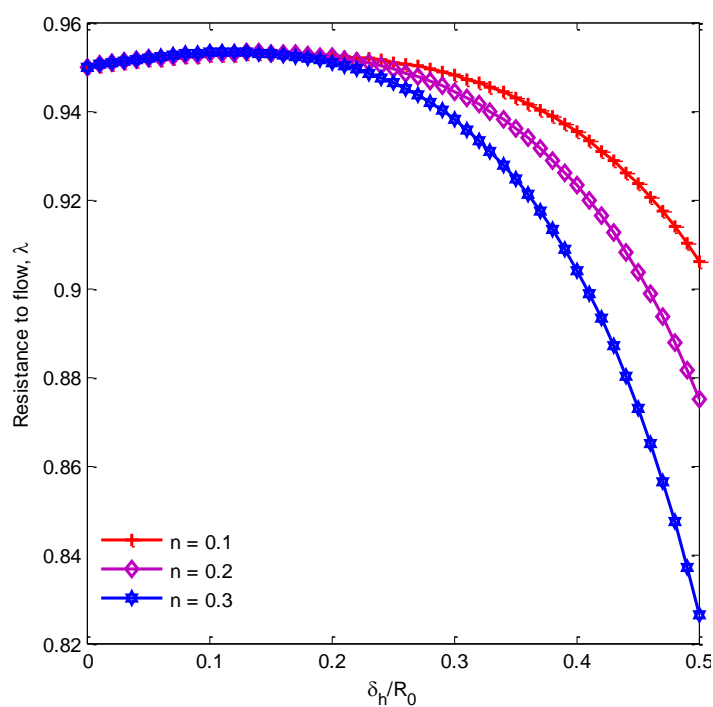


Figure 9: Variation of resistance to flow, $\bar{\lambda}$ with $\frac{\delta_h}{R_0}$ for values of $n = 0.1, 0.2, 0.3$ based on power-law

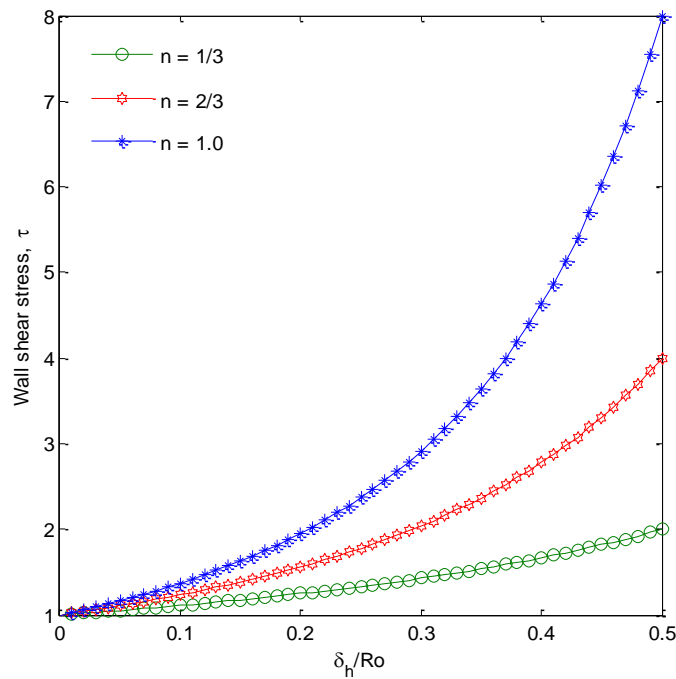


Figure 10: Variation of arterial wall shear stress (pressure) $\bar{\tau}$ with $\frac{\delta_h}{R_0}$ for values of $n=1/3, 2/3$ and 1.0 based on power law fluid

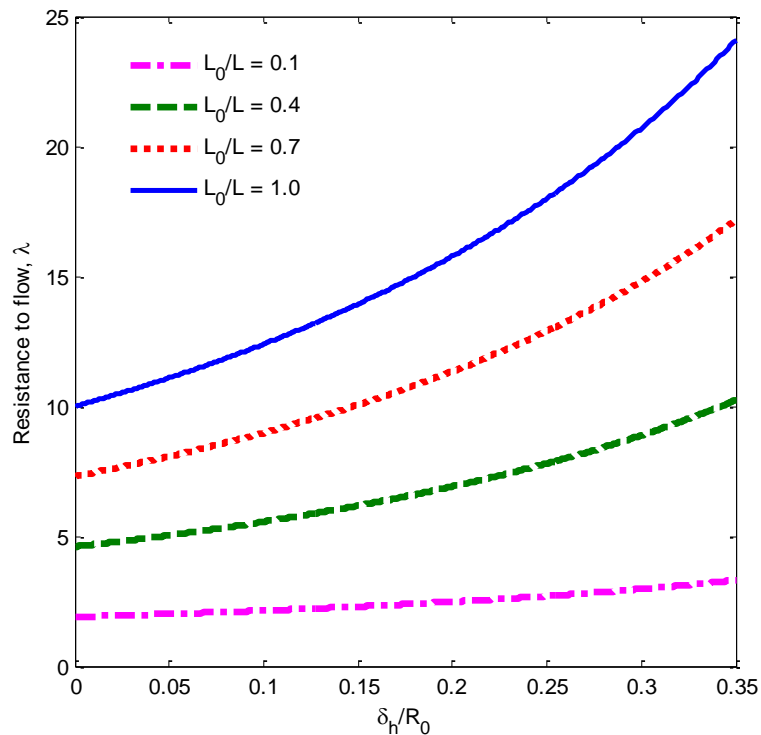


Figure 11: Variation of resistance to flow, $\bar{\lambda}$ with $\frac{\delta_h}{R_0}$ for values of $L_0/L=0.1, 0.4, 0.7$ and 1.0 based on Casson – Fluid

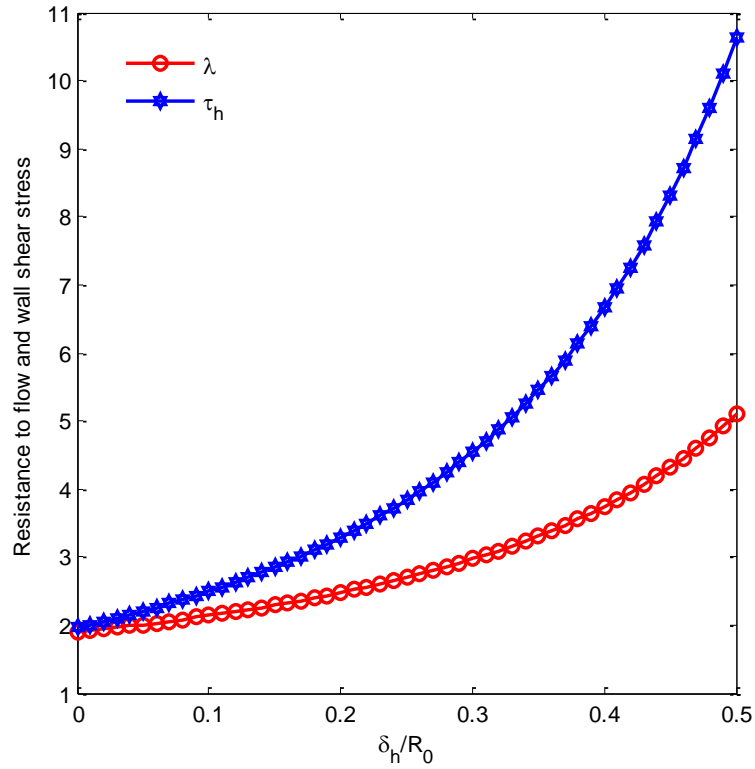


Figure 12: Variation of resistance to flow, $\bar{\lambda}$ and arterial wall shear stress (pressure drop) $\bar{\tau}$ with $\frac{\delta_h}{R_0}$

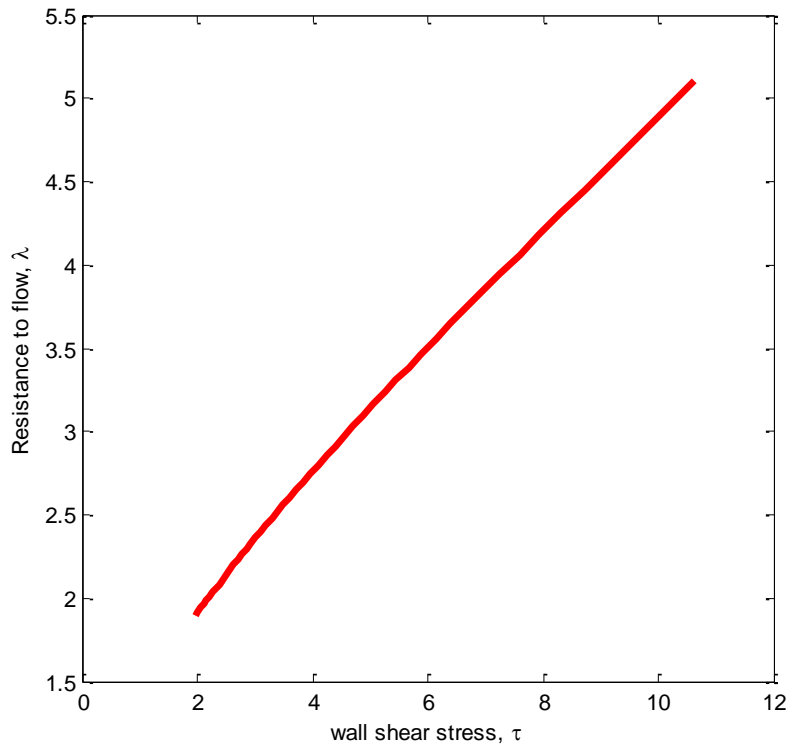


Figure 13: Variation of resistance to flow and arterial wall shear stress

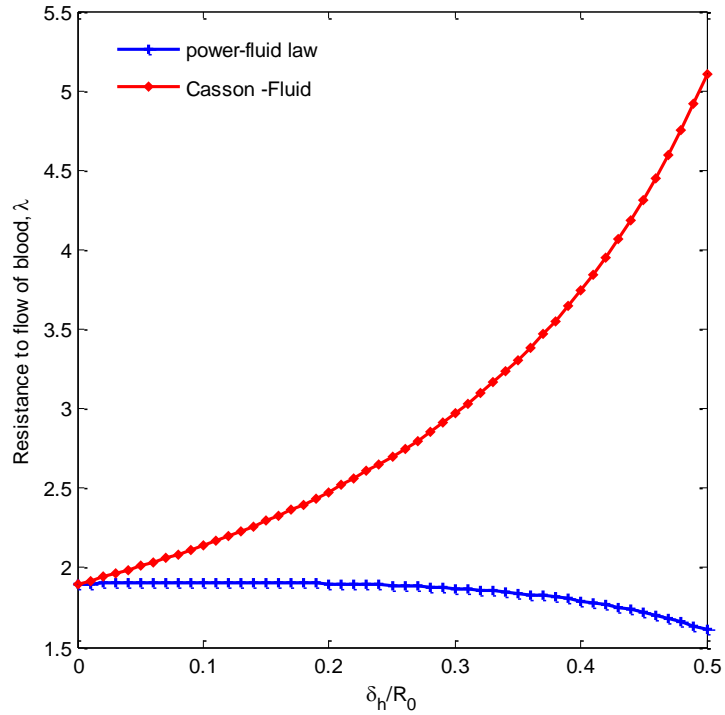


Figure 14: Comparison of the resistance to flow based on both power-fluid law and Casson fluid

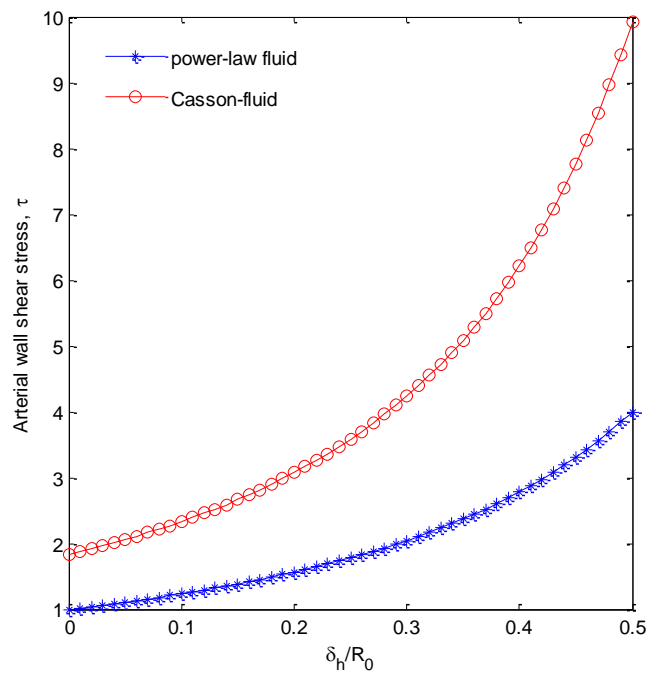


Figure 15: Comparison of the arterial wall shear stress (pressure drop) τ with $\frac{\delta h}{R_0}$ based on both power-fluid law and Casson fluid

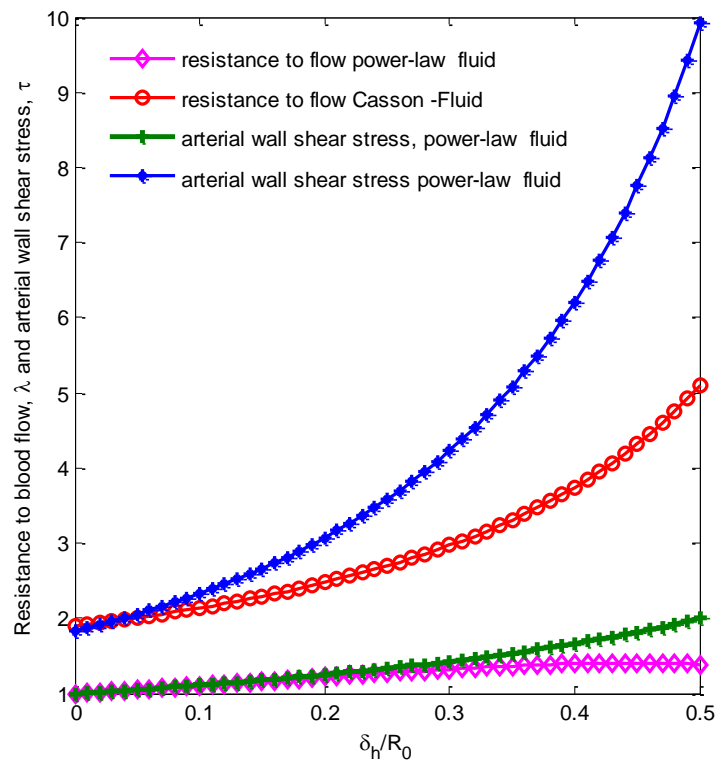


Figure 16: Variation of resistance to flow, $\bar{\lambda}$ and arterial wall shear stress (pressure drop) $\bar{\tau}$ with $\frac{\delta_h}{R_0}$ based on both power-law and Casson fluid

IV. Discussion

The analytic expression for resistance to flow $\bar{\lambda}$ is given by equation (24) for Model I which is based on Power-law fluid. It has been plotted with $\frac{\delta_h}{R_0}$ for different values of n and L_0/L . These results are shown by Figures 8 and 9 respectively. It is evident from Figure 8 that as the size of stenosis increases the resistance to flow increases meanwhile, from Figure 9 it has been observed that resistance to the flow of blood, $\bar{\lambda}$ increases as power-law index, n increases. Further it is noticed that the resistance to flow for $\frac{\delta_h}{R_0} = 0.1$ and $L_0/L = 1.0$ over the normal artery has been increased by 23.9% for Newtonian case ($n = 1$) but only 11.1% for non-Newtonian case ($n = 2/3$).

The arterial wall shear stress is studied in Figure 10 where the variation of arterial wall shear stress (pressure) $\bar{\tau}$ with $\frac{\delta_h}{R_0}$ for values of $n=1/3, 2/3$ and 1.0 based on power law fluid is presented. As the n increases from $1/3$ to 1.0 , the pressure generated at the walls of the artery increased rapidly thereby subjecting the arterial channel to danger of complications which may result to a diseased artery. This result is believed to have agreed with [13] who argues that the normal condition of arteries and blood flow can be affected by vascular diseases. One of the most common vascular diseases that cause serious morbidity and death is atherosclerosis. Atherosclerosis is a disorder characterized by progressive abnormal narrowing and occlusion of the lumen of artery. The narrowing is caused by obstruction or stenosis, which is formed by deposition of fatty substances, cholesterol, cellular waste products, calcium, and fibrin in the inner layer of an artery. As the deposition continues to accumulate, it will build up into plaque. If a piece of plaque breaks away, it can cause bleeding into the plaque. The formation of thrombus (blood clots) around the plaque may cause the condition to get worse.

The resistance to flow given by equation (32), for Model II which is based on Casson fluid have been plotted with $\frac{\delta_h}{R_0}$ in Figure 11. It has been observed that $\bar{\lambda}$ decreases as τ_0 increases. As a result, it increasingly disrupts the blood flow or completely blocks the flow of blood to organs, body tissues and structures. This result is in consonance with [4] who explained further that is particularly dangerous in the coronary and carotid arteries due to the critical oxygen requirement of the heart and brain. The carotid arteries provide blood to the brain, while coronary arteries provide blood to the heart. When the blood supply is limited, patients can suffer

stroke and heart attack, respectively. If renal arteries that supply blood to the kidneys are severely obstructed, there is a serious risk of developing chronic kidney disease.

It is deduced from Figure 12 that as $\frac{\delta h}{R_0}$ increases, the resistance to the flow of blood increases together with the arterial wall shear stress such that at every point, arterial wall shear stress is more than resistance to the flow of blood. This trend informed our study of the variation of resistance to flow with arterial wall shear stress showing that both of them increases with each.

From Figure 14, it is clear that the resistance to the flow of blood is always greater than unity for both power-law and Casson fluid and increases with the size of stenosis. This trend is in consonance with that of the variation in the arterial wall shear stress as shown in Figure 15. These trends in the resistance to flow and arterial wall shear stress are plotted and presented in Figure 16. The results obtained are in good agreement with [2] and [7] for both models.

V. Conclusion

This study investigated a stenosed arterial segment in which the blood is flowing. Blood is represented by two different non-Newtonian fluids namely Power-law and Casson-fluid. The analytic expressions for resistance to flow and wall shear stress have been obtained. From the results obtained in the analysis for various values of the involved parameters, it has been observed that the resistance to flow and wall shear stress increases as the height of stenosis increases but the rate of increase is slower than that of Newtonian models for both the models. Thus, the present models are able to predict some main characteristics of the physiological flows and may be useful for some biomedical applications although the estimation of parameters are taken on the basis of existing literature.

Fluid mechanics of arterial stenosis plays an important role in the early detection of any stroke-related problems associated with cerebrovascular or cardiovascular system [8]. Shear stress and Resistance to flow are the two important parameters associated with the mechanical characteristics of vessel wall. Information pertaining to these two flow variables can be used for the assessment of strength of the affected vessel wall. In view of the above, it is hoped that, the present findings could be useful in the design of flow meters in bio-medical instrumentation.

References

- [1]. Labadin, J. and Ahmadi, A. Mathematical Modeling of the Arterial Blood Flow, Proceedings of the 2nd IMT-GT Regional Conference on Mathematics, Statistics and Applications, Universiti Sains Malaysia, Penang, June 13 – 15, 2006.
- [2]. Padma, J., Ashutosh, P. and Joshi, B.K. Two-Layered Model of Blood Flow through Composite Stenosed Artery, *Applications and Applied Mathematics: An International Journal (AAM)*, 2009; 4 (2): 343 – 354.
- [3]. Ahmed, S. K., Usama, E. G. and Sameh, A. A. Color Doppler blood flow indices of the superior mesenteric artery as an early predictor of necrotizing enterocolitis in preterm neonates, *International Journal of Medical Imaging*, 2014; 2(2): 39-43
- [4]. Levick, J. R. *An Introduction to Cardiovascular Physiology*, 5th Edition. London: Hodder Arnold, 2010.
- [5]. Mbah, G. C. E. and Adagba, H. O. Flow of Blood through a Constricted Capillary. *Journal of Mathematical Sciences*, 2010; 21 (2): 115-126.
- [6]. Misra, J. C. and Shit, G. C., Blood Flow through Arteries in a Pathological State: A Theoretical Study. *Int. J. Engng. Sci.*, 44 Pg. 662-671.
- [7]. Pralhad, R. N. and Schultz, D. H. Modeling of Arterial Stenosis and Its Applications to Blood Diseases. *Mathematical Biosciences*, 2004; 190: 203-220.
- [8]. Shukla, J. B., Parihar, R. S. and Rao, B. R. P. Effects of Stenosis on Non-Newtonian Flow of the Blood in an Artery. *Bulletin of Mathematical Biology*, 1980. 42: 283-294.
- [9]. Stroud, K. A. *Advanced Engineering Mathematics, Fourth Edition*. New York: Palgrave Macmillan. 2003; ISBN 1-4039-0312-3.
- [10]. Tivde, T. and Animalu, A.O.E. Riccati Equations in Biophysics and Other Physical Phenomenon. *African Journal of Physics (AJP)*, 2008; Vol. 1, Pg. 154.
- [11]. Tivde, T. Mathematical Modelling of Blood Flow in the Internal Carotid Artery. LAP LAMBERT Academic Publishing GmbH & Co. KG, 2012; 978-3-659-13738-9.
- [12]. Tivde, T. and Mbah, G.C.E. Modelling of Blood Flow in an Occluded Internal Carotid Artery. *Journal of Scientific Research in Physical & Mathematical Science*, 2015; 2 (7): 14 – 27.
- [13]. Joshi, P., Pathak, A. and Joshi, B. K., Effect of Blood Flow in a Composite Stenosed Artery, *Varahmihir, Journal of Mathematical Sciences*, to appear. 2009

Tivde, T, et.al. "Mathematical Modelling of Arterial Constriction in the Presence of Blood Diseases." *IOSR Journal of Mobile Computing & Application (IOSR-JMCA)*, 8(1), (2021): pp. 08-22.